Acta Crystallographica Section A
Foundations of Crystallography
ISSN 0108-7673

Received 17 August 2012
Accepted 19 November 2012

The significance of Bragg's law in electron diffraction and microscopy, and Bragg's second law

C. J. Humphreys

Department of Materials Science and Metallurgy, University of Cambridge, Pembroke Street, Cambridge CB2 3QZ, United Kingdom

Bragg's second law, which deserves to be more widely known, is recounted. The significance of Bragg's law in electron diffraction and microscopy is then discussed, with particular emphasis on differences between X-ray and electron diffraction. As an example of such differences, the critical voltage effect in electron diffraction is described. It is then shown that the lattice imaging of crystals in high-resolution electron microscopy directly reveals the Bragg planes used for the imaging process, exactly as visualized by Bragg in his real-space law. Finally, it is shown how in 2012, for the first time, on the centennial anniversary of Bragg's law, single atoms have been identified in an electron microscope using X-rays emitted from the specimen. Hence atomic resolution X-ray maps of a crystal in real space can be formed which give the positions and identities of the different atoms in the crystal, or of a single impurity atom in the crystal.

1. Introduction

As William Lawrence Bragg walked along the banks of the River Cam in Cambridge in the autumn of 1912 he had a simple but brilliant idea. An idea which was to transform not only physics, but also materials science, chemistry, geology and biology. He realised that X-ray diffraction by a crystal could be visualized as arising from reflection of the X-rays by planes of atoms in the crystal, hence the arrangement of atoms in a crystal could be determined by observing beams of X-rays reflected from different crystal planes (Bragg, 1912*a*,*b*,*c*). See also Spence (2013).

In this paper I will discuss the role and significance of Bragg's law, $n\lambda = 2d \sin\theta$, in electron diffraction and differences from the X-ray case. I will also discuss the imaging of crystal lattices and atoms in electron microscopy since, like Bragg's law, this occurs in real space and such images are an important direct modern visualization of Bragg's law. However, first I will describe the little-known Bragg's second law, because I believe it deserves to be more widely known and it is particularly appropriate to revive the knowledge of it in this centenary of Bragg's first law.

2. Bragg's second law

The story of Bragg's second law was published by E. W. Hughes in an article entitled *How I first learned of the Patterson function and Bragg's second law* (Hughes, 1987; see also Thomas, 1990). Hughes recounts that Lawrence Bragg was visiting the Department of Chemistry at Cornell University, Ithaca, New York, to deliver the George Fisher Baker Lectures. Hughes had been asked to be his assistant during his visit. It was the late winter of 1933, it had rained all night and then frozen and lightly snowed. The streets were sheets of ice. Bragg asked Hughes if he could drive him to an appointment. Hughes' Model A Ford would not start, so Bragg pushed it while Hughes steered. Eventually the car started and Bragg jumped in. A grit lorry had spread ashes on one side of the road, but not yet on the other side where Hughes was driving.

Hughes recalls that Bragg 'started enthusiastically to tell me about the Patterson method, which he pronounced the most important advance since his father, William Bragg, had introduced the use of Fourier series. He used the fingers of one hand to represent atomic position vectors and those of the other to represent their differences, and I soon forgot all about the ice.' Hughes then recalled that he looked up to see a red traffic light just in front of him at a road junction. Hughes braked, skidded, swerved and crossed the red light, ending up in the road intersection. They were in the path of a heavy lorry which was going fast through its green light. The lorry swerved and missed them by about a foot. Hughes, shaken and stirred, cautiously drove on. He recounts: 'Through all this Bragg continued to wave his hands and lecture on Patterson's vectors, but to a deaf audience!'

Hughes writes that the following year he was in England and this time Bragg was driving him. They passed the scene of a recent bad road accident, which reminded Hughes of what could have happened in Ithaca. So Hughes asked Bragg if he remembered the incident. Bragg replied that indeed he did. He then stated the following, which Hughes calls *Bragg's second law*.

> When travelling in a foreign country I make it a point of personal honour not to show fear, anger, or mirth, or surprise at any happening that does not seem to be unusual to the natives.

Hughes ended his article by saying that he considered this 'law' to be excellent advice which he had tried to follow.

However, he added that on that winter morning in Ithaca, Bragg was not very good at estimating the reaction of the native.

3. Electron and X-ray diffraction: similarities and differences

If we consider the elastic scattering of X-rays or fast electrons by a single atom, it is well known that the atomic scattering factor for X-rays is equal to the Fourier transform of the electron charge density, and the atomic scattering amplitude for electrons (in the first Born approximation) is proportional to the Fourier transform of the atomic potential. Thus the Fourier transform concept is a unifying concept in X-ray and electron diffraction (and also in optical and neutron diffraction).

However, the magnitude of the atomic scattering amplitude for electrons is typically between 1 and 10 Å. This is very much greater than the scattering amplitude for X-rays, $r_e f^x$ (about 10^{-4} Å), where f^x is the atomic scattering factor for X-rays and r_e is the classical electron radius, which is the scaling factor necessary to compare the magnitude of X-ray and electron scattering (see, for example, Humphreys, 1979). Since the scattered intensity is proportional to the square of the scattering amplitude, the intensity of electrons scattered by a single atom is a massive 10^8 times greater that the intensity of X-rays scattered. Hence atoms are weakly scattering objects for X-rays, but strongly scattering objects for electrons. It follows that in an assembly of atoms, such as a crystal, multiple scattering is much more important for electrons than for X-rays.

A second fundamental difference between X-ray and electron diffraction is the wavelength of the radiation used. Although Bragg's law, $n\lambda = 2d\sin\theta$, applies to both X-ray and electron diffraction, the wavelength λ of the radiation used is normally very different. For incident fast electrons, as used in an electron microscope, the Ewald sphere radius of curvature is very large with respect to reciprocal-lattice vectors (for 100 keV electrons, $k = \lambda^{-1} \simeq 27$ Å^{-1}). Since for a thin crystal each reciprocal-lattice point is effectively extended into a spike or rod, many spikes usually intersect the Ewald sphere. Hence a typical electron diffraction pattern, using monochromatic electrons, contains many diffraction spots. For monochromatic X-ray diffraction, on the other hand, the radius of curvature of the Ewald sphere is small (λ is typically about 1 Å, so $k = \lambda^{-1} \simeq 1$ Å^{-1}) and the crystal thickness is relatively large, hence the crystal has to be oriented very carefully to obtain even one diffracted beam.

The two simple differences described above (wavelength and strength of scattering) have profound consequences when comparing electron and X-ray diffraction. For example, multiple scattering is much more important in electron diffraction, extinction distances are much shorter in electron diffraction (see Humphreys, 1979), Bragg peaks are much wider in electron diffraction, diffracted intensities in electron diffraction contain phase information [because of strong multiple scattering, see Moodie *et al.* (1996) and Nakashima *et al.* (2011)], and so on. In order to illustrate the major differences between electron and X-ray diffraction I will now describe a remarkable effect which I believe would have astonished Bragg (but not for long!): if a crystal is set at a Bragg reflecting position, the diffracted beam intensity can be a minimum and not a maximum, independent of the crystal thickness.

4. The critical voltage effect in electron diffraction

If a crystal is set at a Bragg reflecting position, normally we expect the diffracted beam intensity to be strong, unless the crystal thickness is an integral number of extinction distances, owing to the constructive interference of waves scattered in the diffracted beam direction. However, in electron diffraction, for a particular incident electron accelerating voltage, known as the critical voltage, V_c, the diffracted beam intensity is very small, due to destructive rather than constructive interference. The critical voltage is a function of the material, Bragg reflection and temperature used.

This effect was discovered in Japan (Nagata & Fukuhara, 1967; Uyeda, 1968; Watanabe *et al.*, 1968). It was rapidly realised that the critical voltage is very sensitive to low-order Fourier coefficients of the crystal potential, V_g, and hence can be used to measure V_g very accurately (to better than 1%). Comparison of experimental critical-voltage-determined V_g values with theoretical free-atom values therefore gives information on solid-state bonding effects in crystals, Debye temperatures *etc.* (Lally *et al.*, 1972; Watanabe & Terasaki, 1972; Hewat & Humphreys, 1974) and band structures in crystals (Smart & Humphreys, 1978).

The simplest case to consider is a crystal set at a second-order Bragg position, $2g$ (Fig. 1). In the three-beam approximation, we consider only the incident beam and diffraction by crystal planes with reciprocal-lattice vectors g and $2g$. Intensity in the $2g$ beam arises from single scattering involving the electron structure amplitude F_{2g}, and double diffraction involving F_g (from 0 to g to $2g$). Taking into account the phase change on scattering it is evident that, for suitable values of F_g and F_{2g}, the intensity in the $2g$ beam can be a minimum, even though it is at the Bragg position. F_g and F_{2g} are proportional to the electron mass m, and for fast electrons m is relativistic and hence varies with the incident electron accelerating voltage. At a particular voltage, called the critical voltage, V_c, destructive interference occurs and I_{2g}, the intensity of the $2g$

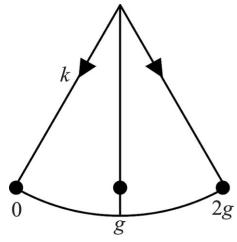

Figure 1
Schematic Ewald sphere construction for a crystal at a second-order Bragg position, $2g$.

beam, is a minimum, even though the crystal is at the Bragg position for this reflection.

It is instructive to consider the critical voltage effect using the Bloch-wave model of electron diffraction. For a crystal set at the second-order reflecting position, three Bloch waves are mainly excited in the crystal. Bloch waves 2 and 3 normally have the strongest excitation amplitudes, and wave 1 the next strongest. The excitations of all other Bloch waves are very small. Below the critical voltage, the kinetic energies of waves 2 and 3 are different and hence their wavevectors are different. As the electron accelerating voltage is raised, the kinetic energies of waves 2 and 3 become more nearly equal until at the critical voltage, V_c, the kinetic energies are identical, hence the wavevectors are equal. This is an accidental degeneracy of the two Bloch waves, and it is very precisely defined. Since one Bloch wave is symmetric and the other is antisymmetric, they interfere destructively and I_{2g} is very small for all crystal thicknesses (there is a small contribution to I_{2g} from Bloch wave 1).

Fig. 2 shows calculated 222 dark-field rocking curves for Cu, at the critical voltage and away from the critical voltage. Away from the critical voltage the I_{222} intensity is a maximum when the crystal is at the exact 222 Bragg position, as expected. However, at the critical voltage the intensity drops to a sharp minimum.

5. Bragg's law and imaging lattice planes in crystals

In an electron diffraction pattern formed in the back focal plane of the objective lens of an electron microscope, the electron wavefunction is the Fourier transform of the electron wavefunction on the exit face of the crystal, and Bragg's law gives the positions of the diffraction spots. However, the electron wavefunction in the image plane in an electron microscope is the Fourier transform of the wavefunction in the diffraction plane (multiplied by a contrast transfer function to take into account apertures and lens aberrations). So the electron wavefunction in the image plane is the Fourier transform of the Fourier transform of the electron wavefunction on the exit face of the crystal, which has the periodicity of the real-space crystal lattice. So the image of a crystal directly reveals the Bragg planes used for the imaging process, if the electron microscope resolution is sufficiently high. Hence, if a crystal is oriented at the exact Bragg position for reflection of the incident electrons by atomic planes of spacing d, the image will directly reveal, appropriately magnified, the atomic planes of spacing d which were used for the imaging (see, for example, Spence, 2008).

Fig. 3 gives an example of such an image, in which the (0002) Bragg reflecting planes in GaN and in InGaN are revealed with their correct lattice spacings, when the electron-microscope magnification is taken into account. Indeed, the electron-microscope magnification is often calibrated by imaging the lattice planes in crystals such as Si, which have well known lattice parameters.

6. Revealing atom column positions using Bragg's law

If a crystal is oriented along a zone axis, then a two-dimensional electron diffraction pattern is produced. If diffracted beams from this two-dimensional pattern are used to form the image, then the positions of atomic columns are

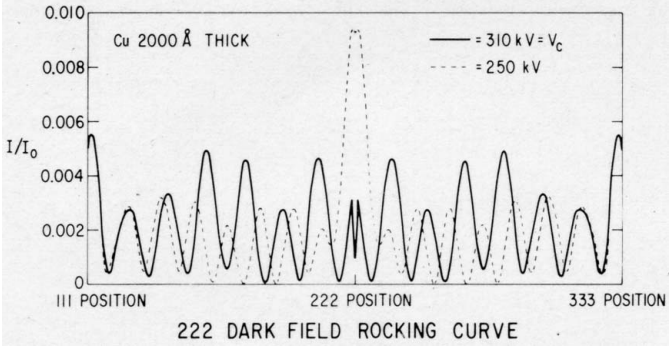

Figure 2
Calculated 222 dark-field rocking curves for a 2000 Å-thick Cu crystal, for incident electron accelerating voltages of 250 kV (dashed curve) and 310 kV (solid curve). Note the minimum 222 intensity when the crystal is at the exact 222 Bragg position for an incident electron accelerating voltage of 310 kV, the critical voltage. Reproduced from Lally *et al.* (1972).

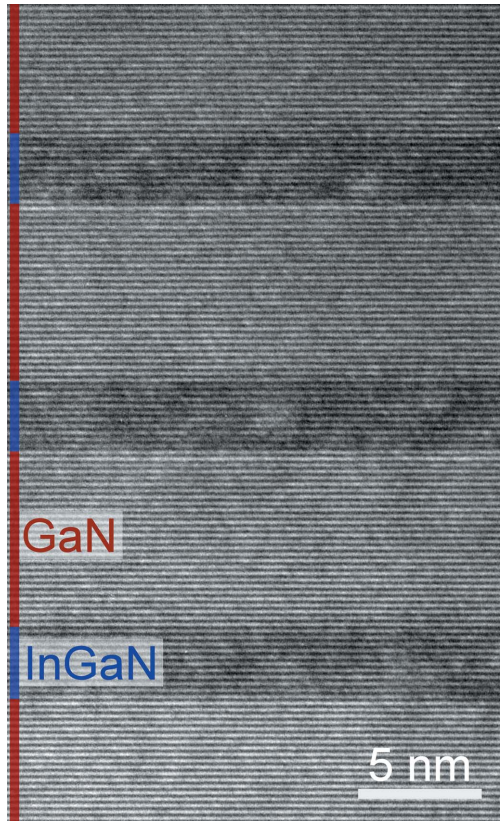

Figure 3
High-resolution transmission electron microscope (0002) lattice fringe image of three InGaN quantum wells separated by GaN barriers. Beams 0 and 0002 were used to form the image. Courtesy T. M. Smeeton.

revealed directly in the image, essentially from where lattice planes cross, again if the electron microscope has sufficient resolution. Aberration correctors are available on modern electron microscopes which correct the aberrations in the objective lens so that the image resolution is better than 1 Å. Aberration correctors are also available which correct the aberrations in the probe-forming condenser lenses so that the incident electron beam can be focused to a spot of less than 1 Å in diameter on the specimen. If this beam is scanned across the specimen, and the high-angle scattered electrons are collected on an annular detector, an HAADF-STEM (high-angle annular dark field scanning transmission electron microscope) image of the specimen is formed in which the columns of atoms in the crystal are directly resolved. InGaN/GaN quantum-well structures, such as shown in Fig. 3, are increasingly being used in light-emitting diodes (LEDs) for solid-state lighting (Humphreys, 2008), with the emitted light coming from the InGaN quantum wells. It has been shown (Watson-Parris *et al.*, 2011) that the electrons in the quantum wells are localized by monolayer-scale well-width fluctuations, whereas the holes are localized by random alloy fluctuations. Fig. 4 shows an HAADF-STEM image of InGaN/GaN quantum wells which have been deliberately grown to have significant well-width fluctuations. It would be extremely difficult, if not impossible, to obtain similar detailed information on well-width fluctuations from X-ray diffraction.

The ability to image individual atomic columns in electron microscopy can yield some unexpected results. In a study of the atomic structure of the AlN on Si interface, an abrupt interface was expected. However, a thin (2 nm thick) amorphous region was unexpectedly found (Fig. 5). (This interface region was confirmed to be amorphous by taking a convergent-beam electron diffraction pattern using a focused probe.) In this projection, the nearest-neighbour Si atoms are resolved (the so-called Si dumbbells) but the nearest-neighbour Al and N atoms are too close to be resolved and hence an Al–N atom pair appears as a single white spot in the image.

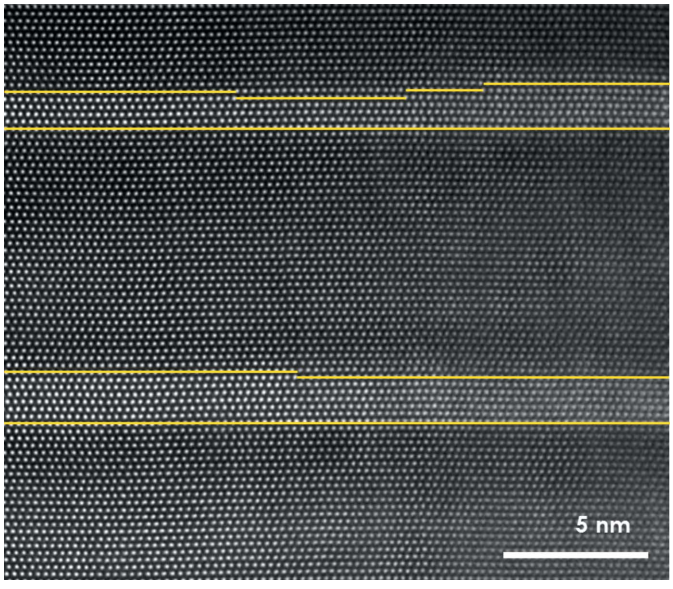

Figure 4
Monolayer thickness steps on InGaN quantum wells (with GaN barriers). Yellow lines outlining the quantum wells have been added to guide the eye. HAADF-STEM image at 300 kV using an aberration-corrected FEI TITAN 80-300 electron microscope. Courtesy S. L. Sahonta.

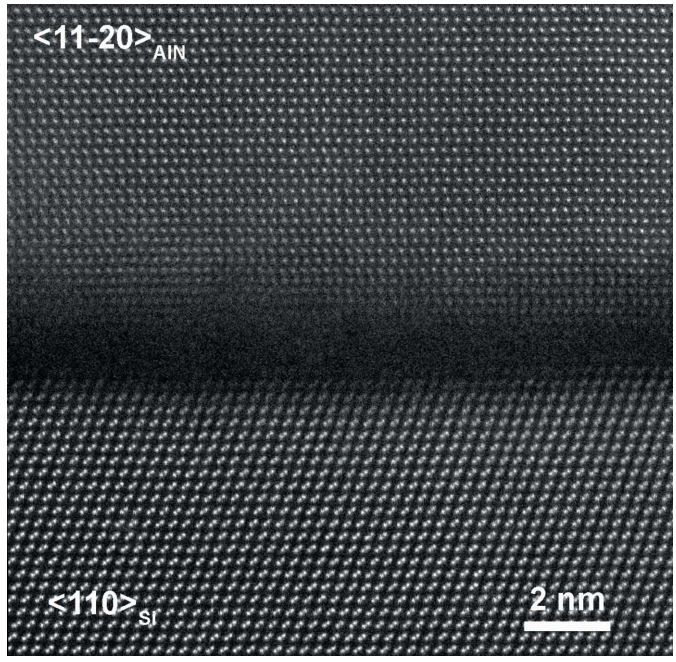

Figure 5
HAADF-STEM image of AlN grown on Si. Note the amorphous region about 2 nm thick at the interface. C_s-corrected FEI Titan 80-300 operated at 300 kV, spot size ~1 Å. Reproduced with permission from Radtke *et al.* (2010). Copyright (2010), American Institute of Physics.

In order to determine the composition of the amorphous interface layer, images were formed using transmitted electrons which had lost energy by exciting Si L_{23}, N K and Al L_{23} electrons in the specimen (Fig. 6). The amorphous layer was hence determined to be Si_xN_y. It is of interest to note that the AlN layer has good crystalline quality and is epitaxially related to the Si substrate, despite the presence of the amorphous layer (Radtke *et al.*, 2010, 2012).

7. Imaging and identifying single atoms using electrons and X-rays

I believe that Lawrence Bragg would have been amazed and fascinated by the developments in X-ray instrumentation by 2012 that enable single atoms to be identified using X-rays. I will give three examples.

Fig. 7(*a*) shows an image of a so-called peapod specimen: a single erbium atom is inside a fullerene cage which is inside a single-wall carbon nanotube. The fullerene cages are about 1 nm apart. A line spectrum was recorded along the yellow dotted line in Fig. 7(*a*). Fig. 7(*b*) shows the energy-dispersive X-ray spectroscopy (EDX) spectrum, and the erbium M and L lines are clearly visible, as well as the carbon K line (blue arrows). Fig. 7(*c*) shows the electron energy-loss spectrometry (EELS) spectrum recorded simultaneously with the EDX

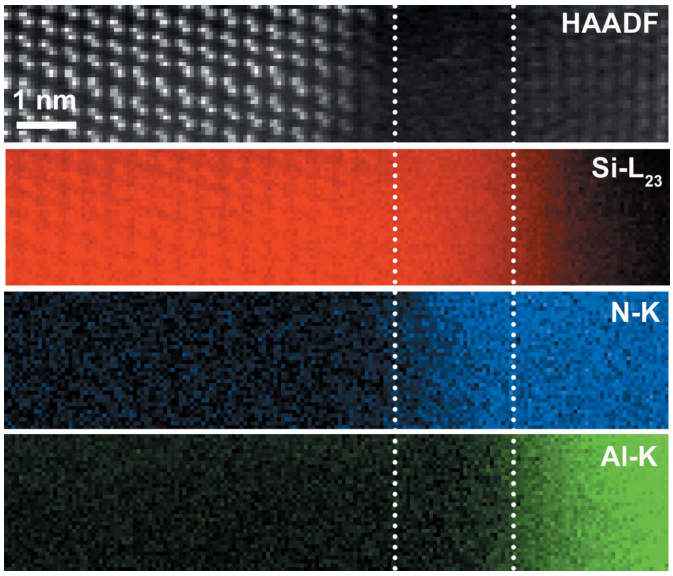

Figure 6
A portion of the image shown in Fig. 5 (rotated through 90°) together with EELS spectral images using electrons which have lost energy by exciting Si L_{23}, N K and Al L_{23} crystal electrons. The dotted lines show the position of the amorphous layer. Reproduced with permission from Radtke *et al.* (2010). Copyright (2010), American Institute of Physics.

spectrum. Although the electron counts in Fig. 7(*c*) are much higher than the photon counts in Fig. 7(*b*), the background in the X-ray spectrum is much lower, so the signal-to-background ratio is higher using X-rays (Suenaga *et al.*, 2012). This single-atom X-ray analysis has been made possible by aberration-corrected electron microscopes with extremely small probes (∼1 Å in diameter), high-brightness field-emission electron sources, and windowless EDX detection using silicon drift detector (SDD) technology, which all lead to significantly higher X-ray count rates than previously.

It is because electrons are scattered strongly, both elastically and inelastically, by single atoms that they can be used to image and analyse single atoms (see §3). A striking example of this is given in Fig. 8, which shows individual carbon atoms clearly resolved in a graphene monolayer, with a single Si atom embedded in it. The impurity atom was identified as Si using simultaneous EDX and EELS. The acquisition time was 4 min and 60 keV electrons were used to minimize radiation damage (Lovejoy *et al.*, 2012).

I believe that Fig. 9 would have particularly interested Lawrence Bragg. It shows atomic resolution X-ray maps (using EDX in an electron microscope) of a GaAs crystal (Watanabe *et al.*, 2012). The Ga $K\alpha$ signal is displayed in green and the Ga atoms are clearly revealed. The As $K\alpha$ signal is displayed in red, and the As atoms are revealed. On the right-hand side of the figure the Ga $K\alpha$ and the As $K\alpha$ signals are overlayed and the X-ray signals from Ga and As atoms are clearly resolved. The top of the figure shows the raw data and the bottom the averaged data.

We should not forget that the X-ray analysis of crystal structures by Lawrence Bragg was highly controversial. Fourteen years after Lawrence had determined the non-

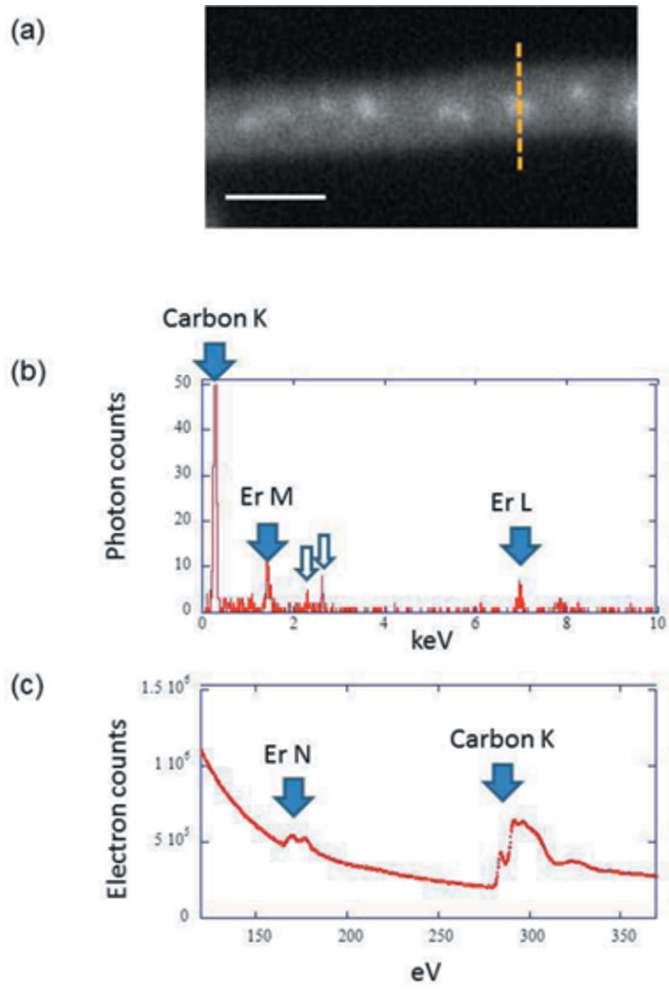

Figure 7
Single-atom EDX and EELS. (*a*) HAADF-STEM image of a peapod specimen: a row of single Er atoms in a C_{82} fullerene cage in a single-wall carbon nanotube. Brighter spots correspond to single Er atoms. 60 keV electrons were used to minimize electron-beam damage in an aberration-corrected Jeol ARM200F. The electron beam was about 1 Å in diameter. (*b*) EDX spectrum recorded from the yellow line scan in (*a*). The solid blue arrows show carbon K and erbium M and L lines. The hollow blue arrows show signals due to the grid and the solvent used in specimen preparation. (*c*) EELS spectrum recorded simultaneously with the EDX spectrum. Adapted from Suenaga *et al.* (2012).

molecular structure of crystalline rock salt (NaCl) (Bragg, 1913), the following astonishing letter appeared in *Nature*, entitled *Poor Common Salt*, by the eminent chemist H. E. Armstrong (Armstrong, 1927):

> On p. 414 [Nature (1927), vol 120], Prof W. L. Bragg asserts that 'In sodium chloride there appear to be no molecules represented by NaCl. The equality in number of sodium and chlorine atoms is arrived at by a chess-board pattern of these atoms; it is a result of geometry and not of a pairing-off of the atoms.' This statement is more than 'repugnant to common sense'. It is absurd to the n . . . th degree, not chemical cricket. Chemistry is neither chess nor geometry, whatever X-ray physics may be. Such unjustified aspersion of the molecular character of our most necessary condiment must not be allowed any longer to pass unchallenged. A little study of the Apostle Paul may be

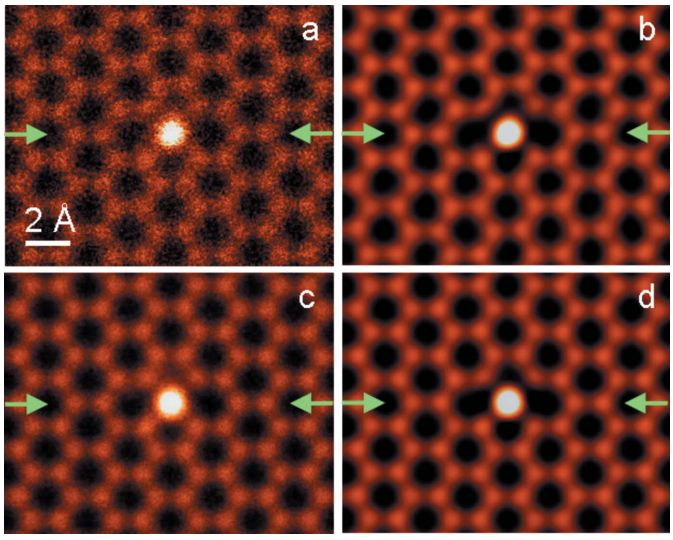

Figure 8
A single Si atom embedded in a graphene monolayer. (*a*), (*b*), (*c*) and (*d*) are images using different HAADF-STEM imaging conditions. Recorded on a Nion UltraStem at 60 kV with a probe size of 1.1 Å. Courtesy W. Zhou, J.-C. Idrobo and O. L. Krivanek.

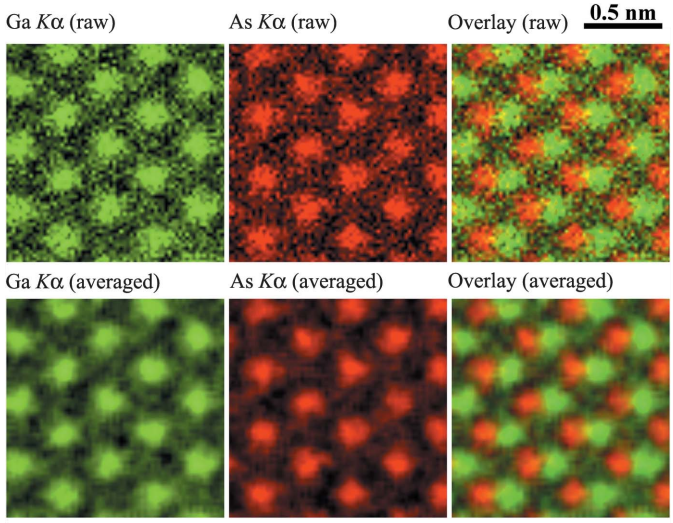

Figure 9
Atomic resolution X-ray maps of GaAs using a Jeol Centurio EDX acquisition system. Courtesy E. Okunishi, JEOL.

> recommended to Prof. Bragg, as a necessary preliminary even to X-ray work, especially as the doctrine has been insistently advocated at the recent Flat Races at Leeds, that science is the pursuit of truth. It were time that chemists took charge of chemistry once more and protected neophytes against the worship of false gods: at least taught them to ask for something more than chess-board evidence.

Fig. 9 clearly demonstrates, in a real-space X-ray map, the 'repugnant' and 'absurd' chess-board pattern of atoms in crystals such as GaAs and NaCl. I believe Lawrence Bragg would have received great pleasure from seeing such an X-ray image. So, one hundred years later, Bragg's real-space vision of using X-rays to determine crystal structures is now being realised in a way he could not have imagined, but in a way he would surely have approved.

References

Armstrong, H. E. (1927). *Nature (London)*, **120**, 478.
Bragg, W. L. (1912*a*). *Proc. Cambridge Philos. Soc.* **17**, 43–57.
Bragg, W. L. (1912*b*). *Nature (London)*, **90**, 402.
Bragg, W. L. (1912*c*). *Nature (London)*, **90**, 410.
Bragg, W. L. (1913). *Proc. R. Soc. London Ser. A*, **89**, 248–260.
Hewat, E. A. & Humphreys, C. J. (1974). *High Voltage Electron Microscopy*, edited by P. R. Swann, C. J. Humphreys & M. J. Goringe, pp. 52–56. New York: Academic Press.
Hughes, E. W. (1987). In *Patterson and Pattersons: Fifty Years of the Patterson Function*, edited by J. P. Glusker, B. K. Patterson & M. Rossi. IUCr Crystallographic Symposia, Vol. 1. Oxford University Press.
Humphreys, C. J. (1979). *Rep. Prog. Phys.* **42**, 1825–1887.
Humphreys, C. J. (2008). *Mater. Res. Soc. Bull.* **33**, 459–470.
Lally, J. S., Humphreys, C. J., Metherell, A. J. F. & Fisher, R. M. (1972). *Philos. Mag.* **25**, 321–343.
Lovejoy, T. C., Ramasse, Q. M., Falke, M., Kaeppel, A., Terborg, R., Zan, R., Dellby, N. & Krivanek, O. L. (2012). *Appl. Phys. Lett.* **100**, 154101.
Moodie, A. F., Etheridge, J. & Humphreys, C. J. (1996). *Acta Cryst.* A**52**, 596–605.
Nagata, F. & Fukuhara, A. (1967). *Jpn. J. Appl. Phys.* **6**, 1233–1235.
Nakashima, P. N., Moodie, A. F. & Etheridge, J. (2011). *Ultramicroscopy*, **111**, 841–846.
Radtke, G., Couillard, M., Botton, G. A., Zhu, D. & Humphreys, C. J. (2010). *Appl. Phys. Lett.* **97**, 251901.
Radtke, G., Couillard, M., Botton, G. A., Zhu, D. & Humphreys, C. J. (2012). *Appl. Phys. Lett.* **100**, 011910.
Smart, D. J. & Humphreys, C. J. (1978). *Electron Diffraction 1927–1977*, edited by P. J. Dobson, J. B. Pendry & C. J. Humphreys, pp. 145–149. Bristol: The Institute of Physics.
Spence, J. C. H. (2008). *High-Resolution Electron Microscopy*. Oxford University Press.
Spence, J. C. H. (2013). *Acta Cryst.* A**69**, 25–33.
Suenaga, K., Okazaki, T., Okunishi, E. & Matsumura, S. (2012). *Nat. Photonics*, **6**, 545–548.
Thomas, J. M. (1990). *Selections and Reflections: The Legacy of Sir Lawrence Bragg*, edited by J. M. Thomas & D. Phillips, pp. 306–308. Northwood: Science Reviews Ltd.
Uyeda, R. (1968). *Acta Cryst.* A**24**, 175–181.
Watanabe, D. & Terasaki, O. (1972). *Proc. Natl Bur. Stand. 5th Mater. Res. Symp.* National Bureau of Standards Special Publication No. 364, pp. 155–158. Washington: US Government Printing Office.
Watanabe, D., Uyeda, R. & Kogiso, M. (1968). *Acta Cryst.* A**24**, 249–250.
Watanabe, M., Yasuhara, A. & Okunishi, E. (2012). *Microsc. Microanal.* **18**, Suppl. 2, 974–975.
Watson-Parris, D., Godfrey, M. J., Dawson, P., Oliver, R. A., Galtrey, M. J., Kappers, M. J. & Humphreys, C. J. (2011). *Phys. Rev. B*, **83**, 115321.